Co 錯体の光誘起原子価異性

崔　愛莉

1. Introduction

Valence tautomerism is characterized by the different species having different distributions of electron density, where metal-to-ligand electron transfer accomplishes interconversion between tautomers. Buchanan et al. reported that a Co complex, [$Co^{II\text{-}HS}$(3,5-dbsq)$_2$(bpy)] (bpy = 2,2'-bipyridine), shows Co-quinone electron transfer in a toluene solution. The intra-molecular charge transfer process can be expressed as

[$Co^{II\text{-}HS}$(3,5-dbsq)$_2$(bpy)] ⇆
[$Co^{III\text{-}LS}$(3,5-dbsq)(3,5-dbcat)(bpy)].

Similar intra-molecular charge transfer has been observed in solid-state Co complexes. Furthermore, it has been reported that charge transfer can be induced by visible light as well as by changes in temperature. Unfortunately, thermal back-transfer of electrons proceeds at an appreciable rate in these systems, limiting their use in practical applications. Here, we describe how the Co compounds, [$Co^{III\text{-}LS}$(3,5-dbsq)(3,5-dbcat)(phen)]·$C_6H_5CH_3$ (**3a**) [$Co^{III\text{-}LS}$(3,5-dbsq)(3,5-dbcat)(tmeda)]·0.5$C_6H_5CH_3$ (**3b**), and [$Co^{III\text{-}LS}$(3,6-dbsq)(3,6-dbcat)(tmpda)] (**3c**), where phen, tmeda and tmpda are 1,10-phenanthrolin, *N,N,N',N'*-tetramethylethylenediamine and *N,N,N',N'*-tetramethylpropylenediamine respectively, show a long-lived intra-molecular charge transfer in response to visible light (Fig. 1). It should be noted that compounds, **3a** and **3c**, have been synthesized by Adams et al. and Jung et al. respectively, and that their basic physical properties have been extensively studied by the same groups.

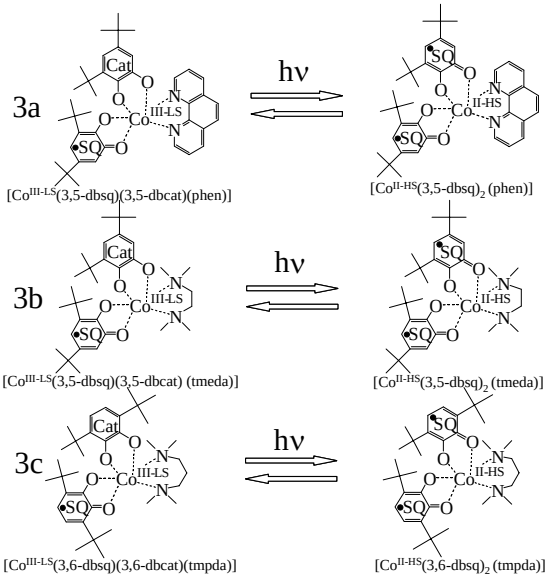

Figure 1. Photoinduced valence tautomerism in Co complexes, **3a** (top), **3b** (middle) and **3c** (bottom).

2. Valence Tautomerism of Co Complexes

The crystal structures of compounds **3a** and **3c** have been reported by Adams et al. and Jung et al., respectively. The space group for each of them is monoclinic ($P2_1/c$).

The μ_{eff} versus T curves, where μ_{eff} is the molar effective magnetic moment and T is the temperature, are shown in Fig. 2. The compounds **3a**, **3b** and **3c** exhibit valence tautomerism at around 240K, 195K and 165 K, respectively. Their valence tautomeric behaviour

[$Co^{II\text{-}HS}$(3,5-dbsq)$_2$(phen)] ⇆
$Co^{III\text{-}LS}$(3,5-dbsq)(3,5-dbcat)(phen)],
[$Co^{II\text{-}HS}$(3,5-dbsq)$_2$(tmeda)] ⇆
[$Co^{III\text{-}LS}$ (3,5-dbsq)(3,5-dbcat)(tmeda)],
[$Co^{II\text{-}HS}$(3,6-dbsq)$_2$(tmpda)] ⇆
[$Co^{III\text{-}LS}$(3,6-dbsq)(3,6-dbcat)(tmpda)],

is consistent with that reported previously. A phase transition accompanies the colour change from dark green-brown at room temperature to blue-black at low temperature. The characteristic absorption band of the high-temperature phase is the $Co^{II\text{-}HS}$ to dbsq (dbsq = 3,5-dbsq and 3,6-dbsq) charge transfer (CT) band observed at around 750~800nm. On the other hand, the low temperature phase has an absorption band at around 600nm, which is characteristic of a ligand field in nature, but it does contain some charge transfer from dbcat (dbcat = 3,5-dbcat and 3,6-dbcat) to $Co^{III\text{-}LS}$. Additionally, in the near-IR region, the phase has a CT band from dbcat to dbsq at around 2500nm.

3. Photoinduced Valence Tautomerism

In order to excite the dbcat to $Co^{III\text{-}LS}$ CT band, the complexes were illuminated in the cavity of a SQUID with 532nm light from a diode pumped Nd:YAG laser. As shown in Fig. 2, the magnetization value increased after illumination. This indicates that the following intra-molecular electron transfer from dbcat to $Co^{III\text{-}LS}$ is induced by the illumination:

[$Co^{III\text{-}LS}$(3,5-dbsq)(3,5-dbcat)(phen)] ->
[$Co^{II\text{-}HS}$(3,5-dbsq)$_2$(phen)]
[$Co^{III\text{-}LS}$ (3,5-dbsq)(3,5-dbcat)(tmeda)] ->
[$Co^{II\text{-}HS}$(3,5-dbsq)$_2$(tmeda)]

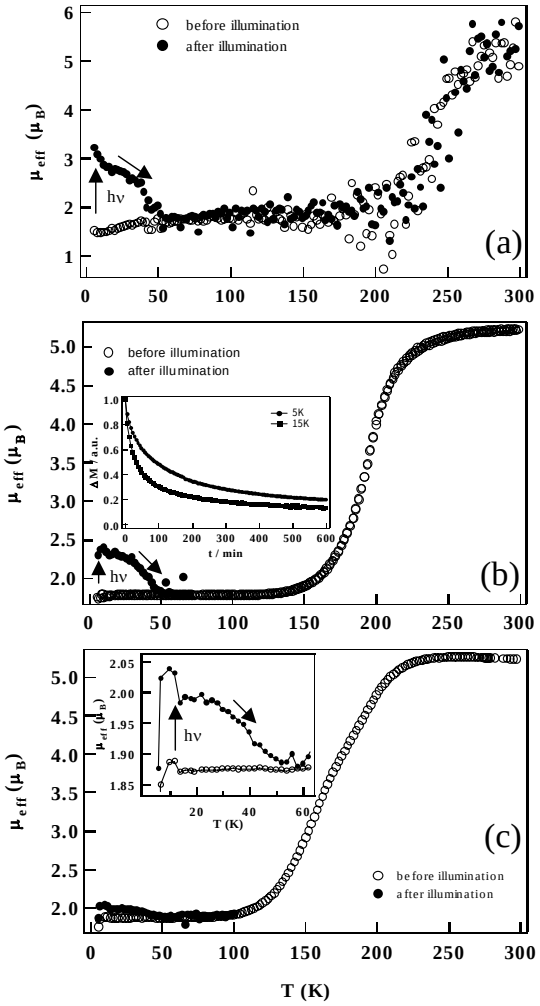

Figure 2. The μ_{eff} versus T plots before (○) and after (●) illumination at 5K for compounds **3a** (top), **3b** (middle) and **3c** (bottom). The sweep rate is 2K min^{-1}.

$[Co^{III\text{-}LS}(3,6\text{-dbsq})(3,6\text{-dbcat})(tmpda)]$ ->
$[Co^{II\text{-}HS}(3,6\text{-dbsq})_2(tmpda)]$

The magnetisation values at 5K after illumination are ca. 2.8, 2.3 and 2.03 μ_B (Bohr Magneton) for **3a**, **3b** and **3c**, respectively. The small magnetization value (2.03 ~ 2.8 μ_B) compared with the value at 300K (5.1 ~ 5.2 μ_B) can be explained by the presence of an antiferromagnetic interaction between $Co^{II\text{-}HS}$ and 3,5-dbsq, and by the overlap of the 3,5-dbcat to $Co^{III\text{-}LS}$ absorption and the $Co^{II\text{-}HS}$ to 3,5-dbsq absorption. The μ_{eff} versus T curve measured at a rate of 2Kmin^{-1} after illumination in the heating mode shows that the metastable state recovered to the original state at around 50K. This means that the lifetime at 50K becomes less than several seconds, which is the time window of our SQUID system.

The absorption spectra of **3a** before and after illumination are shown in Fig. 3. The $Co^{II\text{-}HS}$ to 3,5-dbsq CT band at around 750nm, characteristic of the $[Co^{II\text{-}HS}(3,5\text{-dbsq})_2(phen)]$ state, is significantly increased. It is

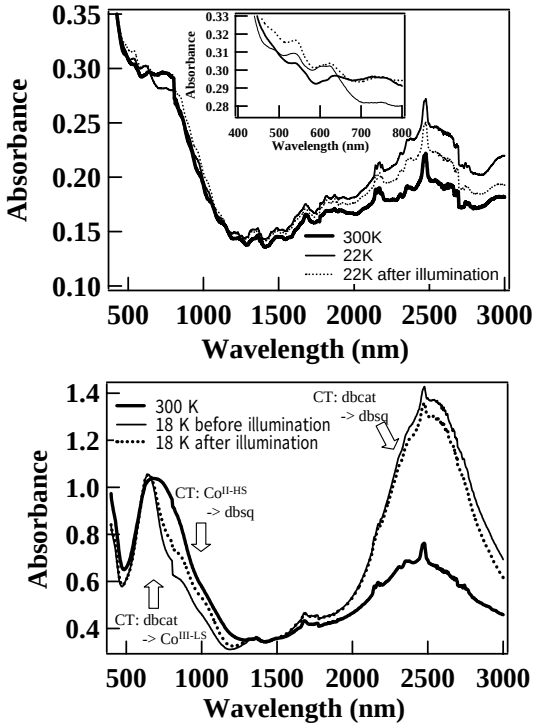

Figure 3. (Top) UV-VIS spectra of **3a** at 300K and 22K before and after illumination. Inset: expanded spectra from 400 to 800nm. (Bottom) UV-VIS spectra of **3b** at 300K, 18K before and after illumination.The μ_{eff} versus T plots before (○) and after (●) illumination at 5K for compounds **3a** (top), **3b** (middle) and **3c** (bottom). The sweep rate is 2K min^{-1}.

found that the absorption spectra after illumination resembles the spectra measured at room temperature. Figure 3 also shows the near-IR spectra before and after illumination. The absorption band at 2500nm, which is ascribable to the CT from 3,5-dbcat to 3,5-dbsq of the $[Co^{III\text{-}LS}(3,5\text{-dbsq})(3,5\text{-dbcat})(phen)]$ state, is reduced after illumination. These spectra show that the CT from 3,5-dbcat to $Co^{III\text{-}LS}$ is induced by light. Similar changes could be observed for **3b** and **3c**.

3．1． **Photoinduced Change in IR, UV-vis and EPR spectra**

The IR spectrum of the Co complex was measured in order to confirm the electronic state of the metastable form. The C-O stretching modes are sensitive to the charge of the ligand moieties. The C=O stretch for free quinone was observed at around 1675cm^{-1}. On the other hand, the peak shifts to lower energy by ca. 60cm^{-1} when the quinone is co-ordinated to a metal ion. Furthermore, when the quinone is reduced to dbsq and dbcat, the stretching mode shifts further to lower frequency. Figure 4 shows that the C-O stretch vibration of dbcat in $[Co^{III\text{-}LS}(dbsq)(dbcat)(NN)]$ (NN = phen, tmeda and tmpda) is observed at 1288, 1280 and 1279cm^{-1} for **3a**, **3b** and **3c**, respectively. On warming, the peak decreased significantly.

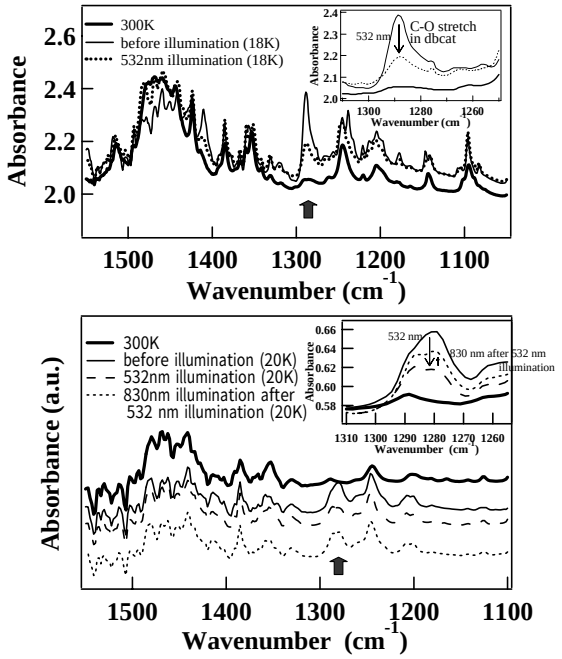

Figure 4. The**.** IR spectra before and after illumination of **3a** (top) and **3b** (bottom). Inset: expanded spectra from 1310 to 1255 cm^{-1}.

This is because dbcat is oxidized to dbsq via thermally-induced valence tautomerism. When the complex, [$Co^{III\text{-}LS}$(dbsq)(dbcat)(NN)], is illuminated at low temperature, the peak at around 1280cm^{-1} is significantly decreased. This is consistent with the proposal that visible light induces charge transfer from dbcat to $Co^{III\text{-}LS}$. When the fraction of the metastable state was estimated from the IR peaks at around 1280cm^{-1}, it was found that about 70 ± 10 % (**3a**), 50 ± 10 % (**3b**) and 10 ± 5 % (**3c**) of the moieties were changed from [$Co^{III\text{-}LS}$(dbsq)(dbcat)(NN)] to [$Co^{II\text{-}HS}(dbsq)_2$(NN)] by illumination. Note that these values are larger than those estimated from UV-VIS spectra. This discrepancy might arise from the different sampling conditions for the two measurements; the IR measurements were performed by the KBr method, while the UV-VIS spectra were measured for a polystyrene film in which the Co complex was embedded. It is thought that the Co complexes are dispersed randomly in the polystyrene film and hence no cooperative interaction operates. If this is the case, the cooperativity due to the intermolecular interaction is essential to achieving photoinduced valence tautomerism. Further study to clarify this problem is in progress.

The X-band EPR spectra also support the occurrence of photoinduced valence tautomerism (Fig. 5). The $Co^{III\text{-}LS}$ complexes with 3,5-dbsq and 3,5-dbcat ligands in a frozen glass typically show a signal centred at g = ca. 2, with eight hyperfine lines due to coupling to the ^{59}Co (I = 7/2) nucleus, while, as powder samples, they do not show the hyperfine coupling with ^{59}Co (I = 7/2). Furthermore, it has been reported

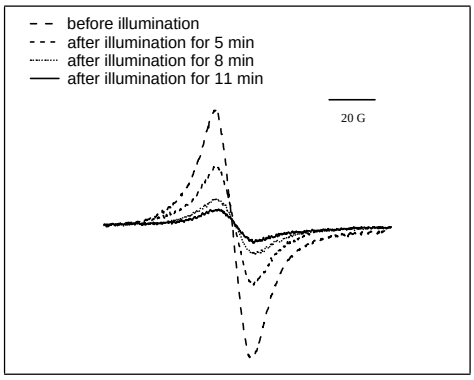

Figure 5. ESR spectra before and after illumination of **3a** at 6K.

that the EPR signal is significantly reduced when the $Co^{III\text{-}LS}$ complexes changed to the $Co^{II\text{-}HS}$ state with two 3,5-dbsq ligands. Figure 5 shows the EPR spectra of **3a** measured at 6K. It exhibits a signal with g values close to 2.00, showing the presence of a one ligand-based radical species. This is consistent with the fact that the Co complex, **3a**, has the electronic state of [$Co^{III\text{-}LS}$(3,5-dbsq)(3,5-dbcat)(phen)] at 6K. The absence of the hyperfine coupling with ^{59}Co (I = 7/2) also agrees with the previous report described above. When the [$Co^{III\text{-}LS}$(3,5-dbsq)(3,5-dbcat)(phen)] complex was illuminated at 6K, the EPR signal was significantly reduced. This change is consistent with the induction of the electron transfer from 3,5-dbcat to $Co^{III\text{-}LS}$.

3. 2. **XANES and EXAFS Measurement**

It is important to note that there is another possible explanation for the photo-induced change in the magnetization. That is, the photo-induced metastable state may have an electronic state of [$Co^{II\text{-}LS}(dbsq)_2$(NN)], not [$Co^{II\text{-}HS}(dbsq)_2$(NN)]. In order to identify the electronic state and local structure around the Co in the metastable state, XANES and EXAFS spectra were measured. Figure. 33 shows the Co *K*-edge XANES spectra of **3a**. The spectra measured at 30 and 300K are consistent with those reported previously. The energy shift originates from the drastic electronic and structural changes around the Co due to thermally induced valence tautomerism. The energy separation of the first intense resonance between 30 and 300K is around 4eV, which is in good agreement with that of the FeCo Prussian blue described above.

When complex **3a** is illuminated with visible light (532 nm) at 11K, a large change in the spectra was observed. As shown in the Fig.6, the spectrum looks like a superposition of the spectrum measured at 30K and the spectrum at 300K, i.e. a superposition of the spectra of the high temperature phase and of the low temperature phase. In fact, the spectrum after

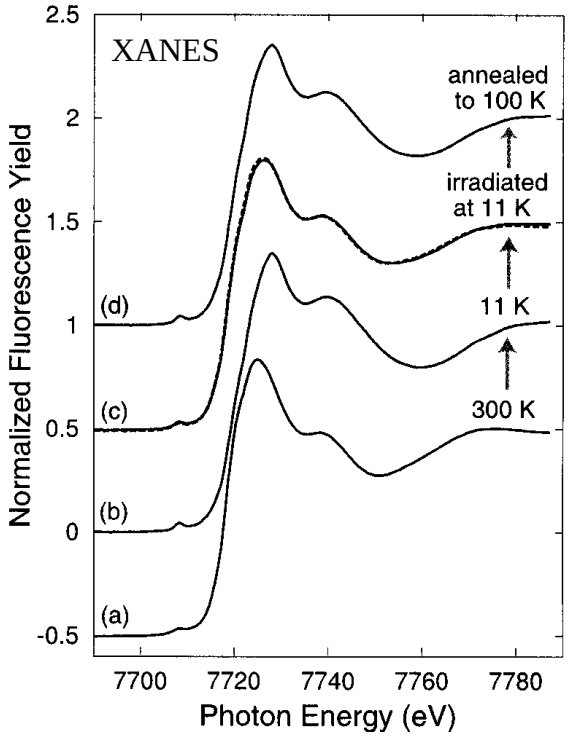

Figure 6. Co *K*-edge XANES spectra taken with the fluorescence-yield mode: (a) 300K; (b) 11K; (c) during visible-light illumination (solid line), together with the simulated spectrum obtained by the superposition of the 300K and 11K spectra with a ratio of 0.65:0.35 (dashed line); (d) after annealing to 100K for the illuminated sample.

illumination could be simulated by summing 65% of the 300K spectrum and 35% of the 30K spectrum. The fact that 65% of the moieties changed to the metastable state is consistent with the value (70 %) estimated from the IR spectra. Thus, it is concluded that the photo-induced trapped excited state is essentially identical to the high temperature phase. Furthermore, the spectrum of the $Co^{II\text{-}LS}$ state should be noticeably different to that of the $Co^{II\text{-}HS}$, as is found in some Co^{II} spin-crossover complexes. This also excludes the possibility of $Co^{II\text{-}LS}$ for the photoinduced metastable state. The changed XANES spectra could be reverted to the original state by heating the sample above 50K, showing that the relaxation involving the electron transfer from $Co^{II\text{-}HS}$ to 3,5-dbsq is thermally induced.

3. 3. Presence of Anti-ferromagnetic Interaction

An important characteristic of the photo-effects described here is that the magnetisation value after illumination does not reach the level observed for $[Co^{II\text{-}HS}(3,5\text{-dbsq})_2(NN)]$ at 300K. In the case of **3b**, the experimental value at 5K after illumination is 2.3 μ_B. On the other hand, at a first glance, the magnetisation value should be 3.5 μ_B, assuming that 50 % of the moieties change to the $[Co^{II\text{-}HS}(3,5\text{-DBSQ})_2(tmeda)]$ state with 5.1 μ_B at 300K. In our opinion, such a small magnetisation value can be explained by the presence of intramolecular magnetic exchange interactions between the dbsq ligands and

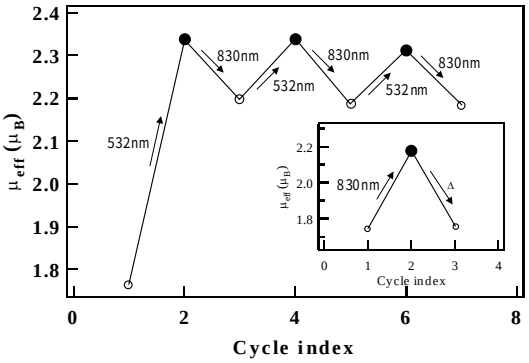

Figure 7. Change in the magnetization by alternate illumination with 532nm light and with 830nm light. Inset: Change in the magnetization induced by illumination with 830nm light and by thermal treatment (Δ) at 60K.

the $Co^{II\text{-}HS}$ ion. In fact, the magnetic interaction of $[Co^{II\text{-}HS}{}_4(3,5\text{-dbsq})_8]$ is anti-ferromagnetic, with an exchange parameter of J = -30 cm^{-1}. Furthermore, it has been reported that the interaction in $[Co^{II\text{-}HS}(3,5\text{-dbsq})_2(phen)]$ can be calculated to be anti-ferromagnetic in nature with J = -594 cm^{-1}. As in the case of those compounds, anti-ferromagnetic interactions are expected between dbsq and the $Co^{II\text{-}HS}$ ion for $[Co^{II\text{-}HS}(dbsq)_2(NN)]$ as follows. The exchange interactions in the compounds under consideration here can be divided into two types. The interaction between the π orbital of dbsq and the e_g orbital of the $Co^{II\text{-}HS}$ is ferromagnetic, because they are orthogonal to each other. The other interaction between the π orbital of dbsq and the t_{2g} orbital of the $Co^{II\text{-}HS}$ gives rise to anti-ferromagnetic character because they overlap with each other. When the ferromagnetic and anti-ferromagnetic interactions are superimposed, the anti-ferromagnetic term, in general, dominates the interactions. The presence of the anti-ferromagnetic exchange interactions gives rise to four different electronic states: one S = 1/2 spin state with the lowest energy, two S = 3/2 states and one S = 5/2 state with the highest energy. Hence, the S = 1/2 state is mainly populated at sufficiently low temperatures due to the Boltzmann distribution. As a result, the magnetisation value after illumination is small compared with that in the high temperature phase.

3. 5. Photoinduced Reverse Valence Tautomerism

The metastable states of **3a**, **3b** and **3c**, $[Co^{II\text{-}HS}(dbsq)_2(NN)]$, have a charge transfer (CT) band from $Co^{II\text{-}HS}$ to dbsq at around 750~800nm. Hence, it might be possible to convert the metastable state back to the ground state by selectively illuminating the metal-to-ligand charge transfer (MLCT) band. In fact, when back electron transfer was investigated for **3b** and **3c**, we found that the metastable states revert to the original ones via reverse electron transfer.

The photoinduced change in the magnetization of **3b** was

shown in Fig. 7. The magnetization value was ca. 2.3 μ_B before the excitation of the MLCT band. When the metastable complex, $[Co^{II\text{-}HS}(3,5\text{-dbsq})_2(tmeda)]\cdot 0.5C_6H_5CH_3$, was illuminated with 830nm light (ca. 30mW/cm^2), the magnetization value decreased. As shown in the figure, the magnetization value after excitation of the MLCT band is ca. 2.2 μ_B. This means that the back electron transfer from the $Co^{II\text{-}HS}$ to the 3,5-DBSQ was induced by light. The photo-process can be expressed as

$[Co^{II\text{-}HS}(3,5\text{-dbsq})_2(tmeda)]\cdot 0.5C_6H_5CH_3$ (metastable state) -> $[Co^{III\text{-}LS}(3,5\text{-dbsq})(3,5\text{-dbcat})(tmeda)]\cdot 0.5C_6H_5CH_3$ (ground state)

The induction of the back electron transfer was confirmed by the UV-vis and the IR spectra. Figure 31 shows the IR spectra measured before and after illumination with 830nm light.

Additionally, it was found that alternate illumination with 532nm and with 830nm light can induce a reversible change in magnetization, as shown in Fig.7.

3. 4. Achievement of a Photo-stationary State

It should be noted that the magnetization value does not reach the original level observed for the pure $[Co^{III\text{-}LS}(dbsq)(dbcat)(NN)]$ state at 5K, i.e. ca. 1.7μ_B. As is described above, the magnetization value of $[Co^{II\text{-}HS}(3,5\text{-dbsq})_2(tmeda)]$ decreased from ca. 2.3 to 2.2μ_B due to 830nm light illumination. This suggests that 70 % of the moieties, whose electronic state was changed from $[Co^{III\text{-}LS}(3,5\text{-dbsq})(3,5\text{-dbcat})(tmeda)]$ to $[Co^{II\text{-}HS}(3,5\text{-dbsq})_2(tmeda)]$ by 532nm light, remain unchanged after illumination with 830nm light. This suggests that the magnetization value, μ_{eff} = ca. 2.2μ_B, is observed as a result of the achievement of the photo-stationary state under the illumination with 830nm light. That is, the excitation at a wavelength of 830nm induces both the LMCT band in the $[Co^{III\text{-}LS}(3,5\text{-dbsq})(3,5\text{-dbcat})(tmeda)]$ (ground state) as well as MLCT band in the $[Co^{II\text{-}HS}(3,5\text{-dbsq})_2(tmeda)]$ (metastable state). In fact, the edge of the LMCT band extends toward a wavelength of 830nm. This is consistent with the observation that, when the complex with the electronic state $[Co^{III\text{-}LS}(3,5\text{-dbsq})(3,5\text{-dbcat})(tmeda)]\cdot 0.5C_6H_5CH_3$ was illuminated with 830nm light at 5K, an increase in the magnetization value from ca. 1.7 to 2.2μ_B was observed (Fig.7). The achievement of a photo-stationary state was also confirmed by an investigation of the wavelength dependence of the photo-effects.

3. 6. Photoinduced Charge Transfer Process

The charge transfer process is illustrated schematically in Fig. 8. The spin-allowed transition, $[Co^{III\text{-}LS}(dbsq)(dbcat)(NN)]$ -> $[Co^{II\text{-}LS}(dbsq)_2(NN)]$, is induced by exciting the CT band from dbcat to $Co^{III\text{-}LS}$. After excitation, some fractions of the excited state relax back to the initial state.

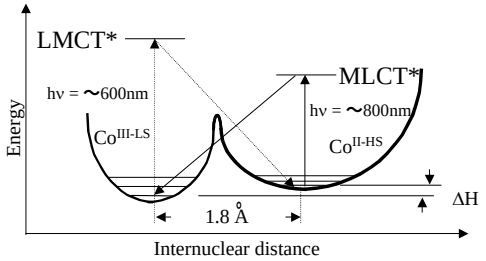

$[Co^{III\text{-}LS}(3,5\text{-dbsq})(3,5\text{-dbcat})(phen)]$ $[Co^{II\text{-}HS}(3,5\text{-dbsq})_2(phen)]$
$[Co^{III\text{-}LS}(3,5\text{-dbsq})(3,5\text{-dbcat})(tmeda)]$ $[Co^{II\text{-}HS}(3,5\text{-dbsq})_2(tmeda)]$
$[Co^{III\text{-}LS}(3,6\text{-dbsq})(3,6\text{-dbcat})(tmpda)]$ $[Co^{II\text{-}HS}(3,6\text{-dbsq})_2(tmpda)]$

Figure 8. Simplified energy-level diagram.

However, an alternative spin forbidden decay path, $[Co^{II\text{-}LS}(dbsq)_2(NN)]$ -> $[Co^{II\text{-}HS}(dbsq)_2(NN)]$, could be possible due to spin-orbit coupling. Consequently, the metastable $[Co^{II\text{-}HS}(dbsq)_2(NN)]$ state can be populated by using visible light. Note that the direct transition from $[Co^{III\text{-}LS}(dbsq)(dbcat)(NN)]$ to $[Co^{II\text{-}HS}(dbsq)_2(NN)]$ is spin forbidden, and hence the process cannot be seen in the spectrum. In a similar manner, back electron transfer could be induced by exciting the MLCT band.

The difference in energy between $[Co^{III\text{-}LS}(3,5\text{-dbsq})(3,5\text{-dbcat})(phen)]$ and $[Co^{II\text{-}LS}(3,5\text{-dbsq})(phen)]$ has been estimated to be 0.278eV, meaning that 26.8 J can be stored per mole. The bottoms of the potential wells for $[Co^{III\text{-}LS}(dbsq)(dbcat)(NN)]$ and $[Co^{II\text{-}LS}(dbsq)_2(NN)]$ were about 0.18Å. The Co *K*-edge EXAFS measurements reveal that the average Co-N,O distances for the high-temperature and low-temperature phases are 2.081Å and 1.904Å respectively. The difference, 0.177Å, is consistent with the above value (0.18Å). It is thought that the existence of two minima in the potential energy curves, with the $[Co^{III\text{-}LS}(dbsq)(dbcat)(NN)]$ state being lower in energy than the $[Co^{II\text{-}LS}(dbsq)_2(NN)]$ state, and the operation of cooperative interactions in the crystal have allowed the observation of the long-lived metastable state.

3. 7. Relevance to Photomechanical Effects and Solar Energy Storage

It is important to note that photomechanical effects involving intramolecular charge transfer have been reported in several compounds. That is, when crystals such as $[Rh^{I}(3,6\text{-DBSQ})(CO)_2]$ and $[Co^{III\text{-}LS}(3,6\text{-dbsq})(3,6\text{-dbcat})(pyrazine)]$ are illuminated, they bend reversibly in response to the light. However, these photomechanical effects can be effectively induced by the near-IR light from a tungsten-halogen lamp, which is different from the present phenomena.

Furthermore, it is interesting to compare the Co valence tautomeric compounds with the layered zirconium phosphonate/viologen compounds. Vermeulen et al. have reported the observation of long-lived charge separation in

zirconium compounds. Although this is quite an interesting system, the charge separation can only be induced by UV-light. Hence, it has been pointed out that the photo-response needs to be moved to longer wavelengths, i.e. the visible region. By contrast, visible light can be used to induce charge transfer in the present Co complexes, so a larger fraction of the solar spectrum can be absorbed. This means that the present Co system will be important from the viewpoint of solar energy storage.

【参考文献】

1. O. Sato, S. Hayami, Z.-Z. Gu, K. Seki, R. Nakajima, and A. Fujishima, Chem. Lett., 874 (2001).
2. T. Yokoyama, K. Okamoto, K. Nagai, T. Ohta, S. Hayami, Z.-Z. Gu, R. Nakajima, and O. Sato, Chem. Phys. Lett. 345, 272 (2001).
3. O. Sato, S. Hayami, Z.-Z. Gu, K. Takahashi, R. Nakajima, K. Seki, and A. Fujishima, J. Photochem. Photobiol. A. Chem. 149, 111 (2002).
4. O. Sato, S. Hayami, Z.-Z. Gu, K. Takahashi, R. Nakajima, and A. Fujishima, Chem. Phys. Lett. 355, 169 (2002).
5. O. Sato, S. Hayami, Z.-Z. Gu, K. Takahashi, R. Nakajima, K. Seki, and A. Fujishima, Phase Transitions, in press.
6. A. Cui, O. Sato, in preparation.
7. 佐藤治　未来材料　2, 38 (2002).